JOURNAL OF GEOPHYSICAL RESEARCH, VOL. 90, NO. C2, PAGES 3161–3172, MARCH 20, 1985

Observations of Surf Beat

R. T. GUZA

Shore Processes Laboratory, Scripps Institution of Oceanography, University of California, La Jolla

EDWARD B. THORNTON

Naval Postgraduate School, Monterey, California

The magnitudes of cross-shore velocity and elevation oscillations at surf beat frequencies observed on three ocean beaches are significantly correlated with the significant height of incident wind waves. Measured surf beat run-up spectra are coupled with numerical integrations of the long wave equations to predict the energy spectrum at offshore sensors, and the coherence and phase between offshore sensors and run-up meter. As in previous studies, valleys in the observed surf beat energy spectra at offshore sensors, and jumps in the relative phase between sensors, occur at the nodal frequencies of simple standing wave (either leaky or high mode edge wave) models. The variance observed in the surf beat cross-shore velocity field is between 10 and 100 times larger near the shoreline than in 5 m depth, and decays more rapidly with increasing offshore distance than the variance in the surf beat elevation field. The standing wave model is qualitatively consistent with this structure.

1. INTRODUCTION

Motions with frequencies substantially lower than that of incident wind generated waves are well known to be important on gently sloping beaches, particularly in the swash region. These oscillations, known as surf beat or infragravity waves, have been observed to contain a substantial portion of the total variance of very shallow water elevation and current fluctuations [*Emery and Gale*, 1951; *Inman*, 1968*a*, *b*; *Suhayda*, 1972, 1974; *Sonu et al.*, 1974; *Goda*, 1975; *Huntley and Bowen*, 1975; *Sasaki and Horikawa*, 1975, 1978; *Sasaki et al.*, 1976; *Huntley*, 1976; *Wright et al.*, 1978, 1979, 1982; *Bradshaw*, 1980; *Holman*, 1981; *Huntley et al.*, 1981; *Guza and Thornton*, 1982]. There is general agreement that wave breaking decreases the energy of swell and wind waves as the shoreline is approached, while surf beat energy levels increase. Surf beat is thought to derive its energy from modulations of the incident wave heights (i.e., beats or groups). In the inner surf zone, the energy at surf beat frequencies can exceed that at wind wave frequencies by at least a factor of four [*Wright et al.*, 1982; *Guza and Thornton*, 1982]. *Holman* [1981] maintained two surf zone current meters during large changes in the incident wave height, and found a correlation between the cross-shore surf beat velocities and visually observed incident wave heights. *Guza and Thornton* [1982] measured run-up surf beat heights at Torrey Pines Beach that were about 70% of the wind wave heights measured directly offshore in 10 m depth. *Munk* [1949] and *Tucker* [1950] found that surf beat heights were about 10% of the wind wave height, with both quantities measured in roughly 15 m depth. *Goda*'s [1975] data showed surf beat heights in about 1 m depth to be between 20% and 40% of the offshore incident wave height.

Several authors have shown varying amounts of agreement between observations of surf beat in the cross-shore velocity and elevation fields, and wave models consisting of high mode edge waves or untrapped "leaky" waves which are standing in the cross-shore direction [*Suhayda*, 1972, 1974; *Huntley*, 1976; *Sasaki et al.*, 1976; *Sasaki and Horikawa*, 1978; *Huntley et al.*, 1981; *Holman*, 1981; and others]. In particular, the observed location of spectral valleys and associated phase jumps in the surf beat cross-spectra generally agree qualitatively with standing wave theory, as does the variation of energy level with offshore distance. In some cases the complicated natural topographies were modeled as a constant slope, so some disparity between theory and observation would be expected even if the basic standing wave hypothesis was completely correct.

There are a few observations of surf beat which have been interpreted to indicate that surf beat is predominantly a progressive wave in the cross-shore direction, rather than a standing wave. Using sensors in about 15 m depth, *Munk* [1949] found a correlation between the surf beat signal and a wind wave related quantity he called the "excess of the shoreward transport over the seaward." The several minute time lag for maximum correlation of the signals suggested that the surf beat signal was primarily a seaward propagating wave radiated by the surf zone. *Tucker* [1950] also concluded that surf beat was a seaward propagating wave, although he deduced this by showing a lagged correlation between surf beat and the envelope of incoming waves, rather than the wind wave "excess transport" used by *Munk* [1949]. Curiously, *Meadows et al.* [1982, Figure 4] used basically the same technique as *Tucker* [1950] but reached a conflicting conclusion. *Meadows et al.* [1982] concluded that surf beat is a shoreward propagating wave 180° out of phase with incoming wind wave groups, rather than an outgoing wave [*Tucker*, 1950]. *Longuet-Higgins and Stewart* [1962] showed theoretically how a shoreward propagating wave might be generated as the nonlinear response to incoming wave groups. However, apparently motivated by *Tucker*'s [1950] observations, *Longuet-Higgins and Stewart* [1962] further hypothesized that the forced long wave is reflected at the beach and that the resulting outgoing wave dominates surf beat fluctuations at offshore locations. It is appropriate to note that in the three experiments where surf beat was suggested to be primarily a progressive wave, no cross-spectra of surf beat at different locations were considered. There was only one surf beat

Paper number 4C1271.
0148-0227/85/004C-1271$05.00

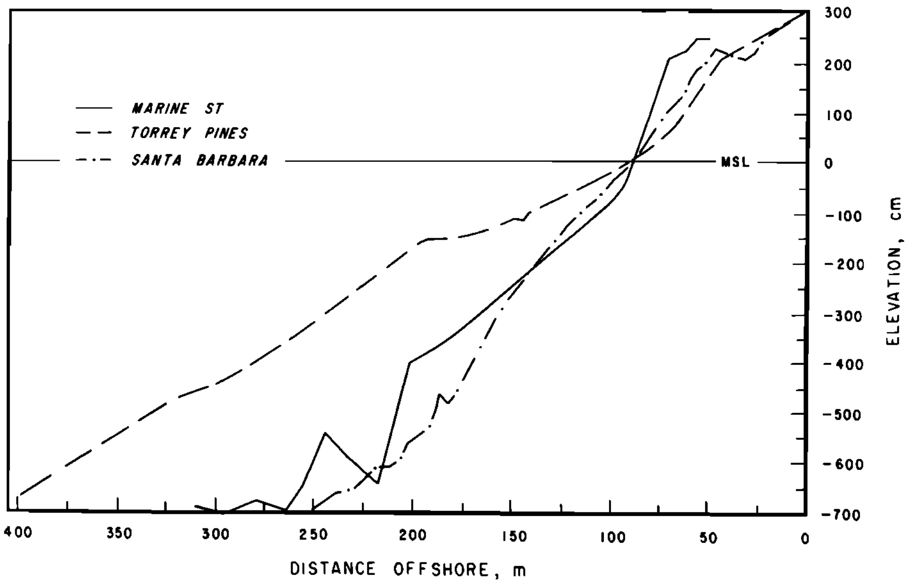

Fig. 1. Typical beach profiles at the study sites. The offshore coordinate origins are selected so that mean sea level (msl) occurs at a common location. Dates of profiles inshore and offshore are: Torrey Pines, November 9, and 18, 1978; Santa Barbara, February 13, 1980, January 22, 1980; Marine Street, February 9, 1981, April 24, 1979.

measurement location in the pioneering studies of *Munk* [1949] and *Tucker* [1950], so the shifting frequencies of spectral extrema and the phase jumps now considered diagnostic of standing waves could not be observed. The conclusions about the progressive nature of surf beat were based on evidence of marginal statistical reliability.

In section 2 a large data set of currents, run-up, and pressure fluctuations is used to further characterize the dependence of surf beat energy levels on incident wind wave conditions. In section 3, solutions are calculated for standing (either high mode edge or leaky) waves by numerical integration of the long wave equations on the observed topography, as suggested by *Holman and Bowen* [1979]. In general, the agreement between observations and standing wave solutions is qualitatively good and similar to previous comparisons [*Suhayda*, 1972, 1974; *Holman*, 1981]. The uniqueness of the present data set is in the range of incident wave conditions, the beach topographies encountered, and in the large number of sensors deployed. Both elevations and currents were measured, and at many more locations than in the previous studies.

2. Surf Beat Energy Levels

Data sets from three different California beaches (Marine Street and Torrey Pines Beaches in San Diego, and Leadbetter Beach in Santa Barbara) are used in the present work. During the Torrey Pines and Santa Barbara experiments, several hours of data were collected daily at high tides for approximately 3 weeks. The sensors used here are on a cross-shore transect extending from the shoreline to about 10 m depth. The number of operational sensors at Torrey Pines and Santa Barbara varied from day to day, but a resistance wire run-up meter, about 12 electromagnetic current meters and 7 elevation (either wave staffs or pressure sensors) gauges were usually operational. Descriptions of the sensors, sensor location maps, and various results of the Torrey Pines experiment are given in *Guza and Thornton* [1980], *Huntley et al.* [1981], *Thornton and Guza* [1982, 1983]. Typical beach profiles are shown in Figure 1. The data runs used here were almost all conducted at tide levels between +120. cm and 0. cm relative to mean sea level. The foreshore slope, based on the portion of the beach extending from a depth of 1 m to the mean shoreline location during the data run was (with one exception) between 0.022 and 0.029 at Torrey Pines. At Santa Barbara, a similarly calculated slope varied between 0.031 and 0.062. To obtain some surf beat data on a steeper beach, a run-up meter and pressure sensor (in 7 m depth) were deployed four times at Marine Street, a coarse-grained beach with a foreshore slope which varied between about 0.06 and 0.12, depending on tide level. In all experiments, rod and level measurements of the foreshore topography were obtained during low tide on the day of each data run. At Torrey Pines and Santa Barbara, topography beyond wading depth was obtained by miniranger surveys both before and after the month long experiments. The offshore ($h > 3$ m) bathymetry for Marine Street was collected 2 years earlier, but spot checks showed no gross changes.

A large amount of data was available. We selected 56 different time periods, of varying duration, for analysis. Time periods were selected so that a wide range of incident wave conditions and foreshore beach slopes were examined. The data for each sensor were screened with various statistical checks and visual inspection of the time series. This tedious and time consuming procedure was particularly important during the larger wave events at Santa Barbara because large drifting kelp mats were sometimes entangled in the current meters, altering the flow field and bending the probes out of alignment. Each time series was then quadratically detrended, an operation which suppressed the variance associated with tidal and other very low frequency fluctuations. The variance remaining at frequencies less than 0.05 Hz was defined as surf beat. The choice of the upper frequency limit for the surf beat frequency band is somewhat arbitrary, and corresponds to the lowest frequency likely to contain significant amounts of energy incident from deep water. On 2 days a long period swell peak at about 0.05 Hz required dropping the upper frequency limit to 0.04 Hz. The energy in the detrended time series, at frequencies less than 0.005 Hz ($T > 200$ s) typically contains less than 10% of the energy in the surf beat band. Most of the surf beat energy, as defined here, is in the fre-

TABLE 1. Data Tabulation

Date	T, min	H_s^{inc}, cm	$H_s^{0,1}$, cm	$H_s^{1,2}$, cm	$U_s^{0,1}$, cm/s	$U_s^{1,2}$, cm/s	R_s^v, cm
			Torrey Pines, November 1978				
4	162	60	19 (1)	19 (3)	88 (2)	53 (3)	
6	102	57	29 (1)	22 (3)	87 (2)	52 (5)	56
7	111	51	15 (1)	15 (3)	64 (1)	43 (5)	37
8	145	61	13 (1)	15 (2)	67 (3)	46 (3)	
10	102	96		27 (2)	114 (3)	89 (4)	73
11	68	117		27 (2)	108 (4)	88 (3)	
12	141	136		37 (1)	144 (1)	120 (4)	103
14	94	72		18 (1)	80 (1)	57 (4)	66
15	94	67	47 (1)	20 (1)	82 (1)	64 (3)	63
17	60	65		22 (2)		49 (4)	54
19	128	61	21 (1)	18 (2)	96 (2)	51 (3)	54
21	68	86	25 (2)	32 (2)	95 (3)	70 (4)	77
22	68	80	21 (1)	21 (3)	119 (1)	77 (5)	68
			Marine Street, February 1981				
9	30	135					85
11	68	90					104
12	68	104					106
12	34	108					102
16	77	117					169
			Santa Barbara, January-February 1980				
Jan. 30	94	28		7 (2)	26 (1)	12 (3)	16
Jan. 31	26	21		5 (1)	22 (3)	10 (6)	8
Feb. 1	68	20		4 (2)	28 (3)	11 (6)	11
2	111	53		24 (2)	118 (3)	52 (8)	46
3	68	74	47 (1)	39 (2)	150 (7)	105 (5)	123
4	256	80	44 (1)	37 (2)	138 (6)	108 (6)	96
5	94	57	46 (1)	28 (2)	100 (7)	75 (5)	82
6	162	40	15 (2)	12 (1)	60 (10)	35 (2)	49
7	94	51	31 (2)	24 (2)	92 (8)	60 (1)	63
8	68	44	44 (1)	21 (1)	114 (4)	63 (1)	
9	51	39	24 (1)	18 (1)	110 (2)	53 (1)	67
10	128	44		20 (2)	97 (6)	49 (5)	
11	68	59		31 (1)	90 (3)	52 (1)	
12	60	44	26 (2)	18 (1)	106 (7)	53 (1)	
13	60	69		13 (2)	71 (2)	38 (6)	
13	60	81		17 (1)	64 (3)	54 (5)	
13	60	92		17 (1)	82 (3)	66 (5)	
13	136	85	20 (1)	19 (3)	91 (4)	60 (6)	
14	85	86		31 (1)	125 (1)	93 (7)	
14	68	87		27 (2)	125 (4)	93 (5)	119
14	77	81	32 (3)	29 (1)	130 (6)	83 (5)	
15	85	73	40 (2)	31 (1)	120 (4)	78 (4)	88
15	55	58	30 (5)	23 (1)	105 (9)	64 (5)	
16	68	115		39 (2)	128 (1)	109 (4)	
16	68	172	26 (2)	39 (2)	137 (2)	113 (2)	
16	68	141		34 (2)	115 (4)	100 (1)	
16	77	123	30 (2)	33 (1)	134 (3)	107 (6)	
16	60	106	32 (3)	30 (1)	122 (2)	99 (6)	
17	77	91	34 (2)	27 (1)	124 (3)	93 (8)	
17	77	102		37 (3)	127 (1)	110 (5)	
17	77	116				121 (4)	
17	77	132		41 (1)		135 (4)	
17	51	139		46 (1)		168 (4)	
17	68	130	56 (1)	52 (2)		131 (2)	
17	171	140		56 (1)		120 (3)	
18	239	128	53 (1)	45 (1)			
18	188	97	37 (1)	29 (2)			
19	179	166		61 (2)			
19	119	188	77 (1)	66 (2)			

quency range 0.005–0.05 Hz. The detailed structure of energy spectra in this frequency range (Figures 4–7) and the spatial variation of energy at fixed frequencies (Figures 8, 9) are discussed later.

The band passed variances at surf beat frequencies ($f < 0.05$ Hz) for each sensor were converted to a "significant" height (or cross-shore velocity) with the definition $H_s = 4\sigma$, where σ^2 is the variance, and U_s is defined analogously. In the present context, H_s and U_s can be considered characteristic magnitudes of elevation and velocity fluctuations associated with surf beat. In order to collapse data from many sensors into a few values representative of the surf zone, significant velocities from sensors in depths less than 1 m were averaged together, as were the significant velocities of sensors in depths between 1 and 2 m. The significant heights were similarly averaged, with the exception of the run-up meter, which was not averaged with any other sensors. The run-up gauge consists of two resistance wires supported a few centimeters (nominally 3

TABLE 2. Relationships Between Significant Surf Beat Quantities and H_s^{inc}

	corr	d.f.	b
$U_s^{1,2}$	0.87	46	0.92 ± 0.04
$U_s^{0,1}$	0.65	40	1.22 ± 0.10
$H_s^{1,2}$	0.86	49	0.32 ± 0.02
$H_s^{0,1}$	0.54	26	0.37 ± 0.05
R_s^v	0.78	25	1.0 ± 0.09

Here, corr is the correlation coefficient, d.f. the degrees of freedom, and b the slope of the best fit line U_s (or H_s) $= bH_s^{inc}$ with cgs units; 90% confidence intervals on b are given.

cm) above the beach face. The run-up meter measures the location, in the plane of the beach face, shoreward of which the water depth is less than (nominally) 3 cm. An intercomparison experiment between the run-up meter and run-up films is discussed in *Holman and Guza* [1984]. These results suggest that run-up variance levels (but not spectral shape) depend on the wire elevation. Using the measured beach profile the run-up time series was converted to a vertical coordinate, detrended, and a "significant vertical run-up excursion" (R_s^v) calculated from the band passed variance. Incident wind wave heights were obtained from the deepest pressure sensor, roughly 10 m depth at Torrey Pines and Santa Barbara, 7 m at Marine Street. The measured pressure spectra were converted to elevation spectra with the use of linear theory. A significant incident wind wave height (H_s^{inc}) was then obtained from the band passed variance in the frequency range 0.05–0.3 Hz. Table 1 shows the date and record length of each run, H_s^{inc}, and the average significant surf beat heights and velocities for each depth category (for example, $U_s^{0,1}$ is the average significant velocity in depths between 0. and 1. m). In Table 1, only H_s^{inc} contains information about wind wave frequencies. The number of sensors used for each average is indicated in parenthesis. About 2000 sensor/hours of data are used here.

The five significant quantities (R_s^v, $H_s^{0,1}$, $H_s^{1,2}$, $U_s^{0,1}$, $U_s^{1,2}$) were each found to be significantly correlated (at the 99.5% level) with H_s^{inc}. The strongest correlations (Table 2) occur in the data obtained in the 1.-2 m depth range ($U_s^{1,2}$, $H_s^{1,2}$). The degrees of freedom in Table 2 are based on the number of (averaged over sensors) significant heights or velocities. Motivated by previous observations and the theoretical suggestion that surf beat heights depend approximately linearly on incident wave heights [*Holman*, 1981], each surf beat parameter was also linearly regressed against H_s^{inc} and the resulting coefficients are shown in Table 2.

Goda's [1975] data showed surf beat heights in about 1. m depth to be between 20% and 40% of the incident wave height, a ratio consistent with the present observations (Table

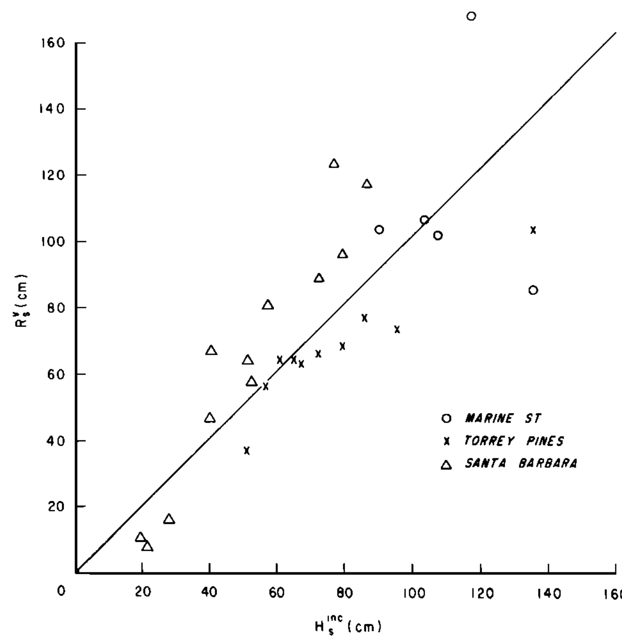

Fig. 3. Significant vertical swash excursion R_s^v versus H_s^{inc}. Solid line is the best fit straight line constrained to pass through the origin, R_s^v (cm) = 1.00 H_s^{inc} (cm).

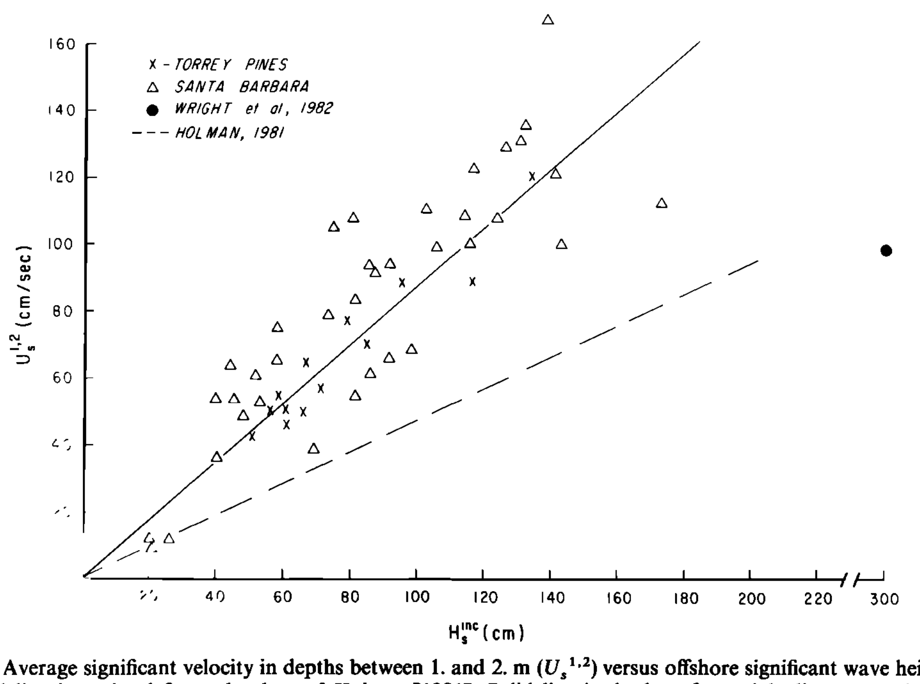

Fig. 2. Average significant velocity in depths between 1. and 2. m ($U_s^{1,2}$) versus offshore significant wave height (H_s^{inc}). The dashed line is a visual fit to the data of *Holman* [1981]. Solid line is the best fit straight line constrained to pass through the origin, $U_s^{1,2}$ (cm/s) = 0.92 s^{-1} H_s^{inc} (cm).

2). The scatter plots of $U_s^{1,2}$ and R_s^v as functions of H_s^{inc}, and the best fit lines, are shown in Figures 2 and 3. Note that there were no current meters at Marine Street, so no data from the steepest beach is included in Figure 2. The slope of the best fit line to $U^{1,2}$ is about twice as large as that reported by *Holman* [1981], on a beach with topography similar to Torrey Pines. It is possible that some of the difference results from a bias in Holman's visual observations of H_s^{inc}. Our own visual observations of H were almost always substantially higher than the values of H_s^{inc} obtained by offshore pressure sensors. It is probably true that visual observations reflect the heights of the largest waves near the breaker line. Thus the visual estimate of H_s^{inc} by *Wright et al.* [1982] may also be biased high (Figure 2). Given the different ways of measuring H_s^{inc}, the existing data suggest that surf beat energy levels (on long, relatively straight beaches with low to moderate slopes) are not extremely sensitive to details of beach morphology or incident wave spectral shape.

Although there are not order of magnitude differences in the depth categorized surf beat energy levels for the same incident wave height, there is very considerable scatter (Figure 2, Table 2). Some is due to variations (between runs) in the precise locations and number of sensors in a given depth range. On any particular day, values from sensors within a given depth range vary by at least a factor of 2, so the depth categorized values are influenced by the details of sensor placement. There are, however, more fundamental effects associated with variations in beach slope. As discussed in more detail below, if the surf beat run-up height depend linearly on incident wave heights (independent of beach slope), then long wave theory suggests that offshore depth categorized quantities ($U_s^{0,1}$, $H_s^{0,1}$) must be functions of beach slope. On the other hand, very recent work (Holman and Sallenger, in press) suggests that the ratio of surf beat run-up to incident wave heights is itself a function of beach slope and incident wave period. Further work is clearly needed to suggest the way to combine incident wave and beach morphology parameters into nondimensional forms which more meaningfully relate incident wave conditions and surf beat energy levels at different offshore locations. The data base presented here may be useful for such studies.

It should also be noted that the present discussion and results (Table 2 and Figures 2 and 3) are based principally on situations in which the incident wave energy peak was in the the range 0.05–0.15 Hz. The upper limit of the surf beat band (0.05 Hz here and in *Holman* [1981]), should clearly be different in a locally wind driven sea with a spectral peak at, say, 0.3 Hz. "Surf beat" is a genetic term implying low frequency energy with an origin in nearshore nonlinear interactions involving higher frequency wind and/or swell waves. Thus the definition of the surf beat frequency band is implicitly based on the incident swell and wind wave spectrum. This is an easy concept to implement when the wind wave spectrum is known a priori, as in a model. In field situations, however, a single frequency band (say, 0.05 Hz) may be composed of both incident waves impinging from deep water and surf beat generated by groups of higher frequency waves (say, 0.2 Hz). There is presently no clear way to separate the two types of motion in real data. The definition of surf beat energy as being in a single frequency band is expedient. However, a background level of long swell could be wrongly identified as surf beat. On the other hand, surf beat excited by wind chop could be at frequencies above the defined surf beat band, resulting in erroneously low calculated values of surf beat energy. The extent to which the present definition of surf beat ($f < 0.05$ Hz) corresponds to the implicit genetic definition is unknown. A precise, operational definition of surf beat is clearly desirable.

3. STANDING WAVES ON A BEACH

Theory

The linear shallow water equations are commonly used to model infragravity waves in the nearshore [*Suhayda*, 1972, 1974; and many others]. With x positive and increasing in the seaward direction, y the longshore coordinate, g gravitational acceleration, h the still water depth, and subscripts indicating differentiation with respect to that variable, the equation for the velocity potential is

$$-\phi_{tt}/g + (h\phi_x)_x + (h\phi_y)_y = 0 \qquad (1)$$

The sea surface elevation η and x and y components of velocity (u, v) are given by

$$\eta = -\phi_t/g \qquad u = \phi_x \qquad v = \phi_y \qquad (2)$$

For a plane beach, $h = x\beta$, simple analytic solutions are known for both edge waves [*Eckart*, 1951] and normally incident waves (here called "leaky" waves) which are totally reflected at the shoreline [*Lamb*, 1932]. For surf beat frequencies, unless the sensors are far offshore, the cross-shore velocity and elevation fields are so similar for high mode edge waves and leaky waves that it is immaterial which solution is used [*Guza*, 1974; *Holman*, 1981]. Leaky wave solutions are used here. *Holman* [1981] and *Huntley et al.* [1981] both suggest that low mode edge waves are not an important component of the surf beat elevation and cross-shore velocity fields.

Holman and Bowen [1979] discuss solutions obtained through numerical integration of (1), and demonstrate that natural beach topographies cannot usually be accurately modelled as a single plane. The complexity of the present topographies (Figure 1) suggested that numerical solutions would be appropriate for comparisons of data and standing wave solutions. Equation (1) was numerically integrated, starting at the shore ($x = 0$), with a scheme known as "repeated extrapolation to the limit" [*Stoer*, 1972]. Time periodicity with radian frequency σ was assumed, the longshore wave number was set equal to zero (the solutions are leaky) and the velocity potential at $x = 0$ obtained by expanding the depth and ϕ in the form

$$h = \beta_1 x + \beta_2 x^2 + \cdots \qquad (3a)$$

$$\phi = \phi_0(1 + \gamma_1 x + \gamma_2 x^2 + \cdots) \qquad (3b)$$

Following *Holman and Bowen* [1979] and equating coefficients of powers of x in (2) yields the following initial conditions:

$$\phi(0) = \phi_0 \qquad (4a)$$

$$u(0) = \phi_x(0) = -\sigma^2\phi_0(g\beta_1)^{-1} \qquad (4b)$$

$$u_x(0) = \phi_{xx}(0) = (\sigma^2(g\beta_1)^{-1})^2(\beta_2 g\sigma^{-2} + 1/2)\phi_0 \qquad (4c)$$

The accuracy of the numerical scheme was confirmed by comparison to analytic leaky wave solutions for topographies with a single slope [*Lamb*, 1932], and two slopes [*Suhayda*, 1972].

Beach slopes for the numerical integrations on real topography were calculated from the beach profile measurements using

$$\beta(x_0) = \left(h\left(x_0 + \frac{\Delta x}{2}\right) - h\left(x_0 - \frac{\Delta x}{2}\right)\right)\Big/\Delta x \qquad (5)$$

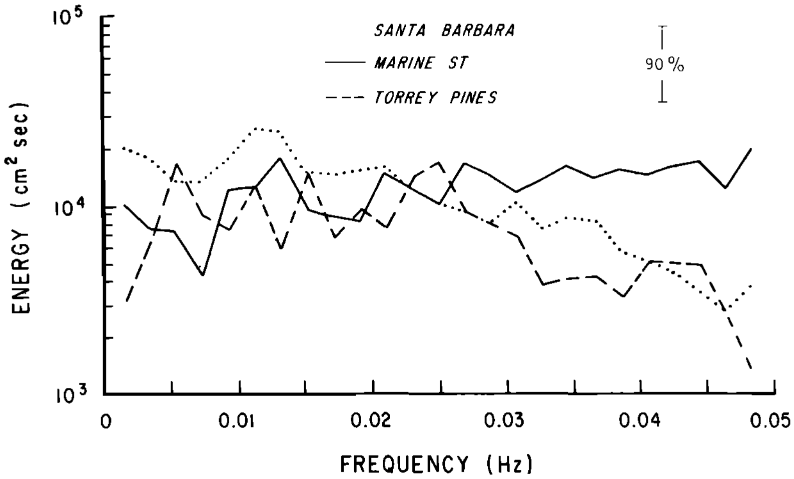

Fig. 4. Vertical run-up spectra for February 11, 1981, Marine Street; November 21, 1978, Torrey Pines; February 4, 1980, Santa Barbara. Degrees of freedom (d.f.) are 16, 16, 60, respectively. The confidence level shown is 90% for 16 d.f.

where x_0 is the location where the beach slope is desired, Δx is a horizontal distance, and depths (h) were obtained by linear interpolation between profile measurements (typically 2 m apart on the foreshore). During the course of performing the integrations on many different natural topographies, with $\Delta x = 2$ m, a few cases arose in which rather different theoretical results were obtained on seemingly similar topographies. These differences are due to the sensitivity of the velocity at $x = 0$ to the shoreline beach slope (β_1 in (4*b*)). Note that if β varies rapidly around $x = 0$, then the choice of Δx in (5) will strongly influence the value of β_1 used in the velocity boundary condition (4*b*). Based on the heuristic argument that small scale topographic variations are not important to long waves, $\Delta x = 40$ m was used in all the calculations presented here. Topographic conditions which resulted in a strong dependence on Δx, usually a short segment of low slope at the mean shoreline, occurred infrequently in the present data set. When the choice of smoothing scale had a substantial influence, solutions based on $\Delta x = 20$–40 m agreed best with the data.

We note that in the numerical solutions of *Holman* [1981] the beach profile measurement points were far enough apart to suppress any rapid variations in beach slope associated with small scale topographic features which may have been present. The spacing of the profile points implicitly smooths the resulting beach slopes. This is obviously desirable at very small scales. For example, the beach slope (and theoretical long wave velocity field) on a rippled bed would show rapid spatial fluctuations much larger than the mean. In some studies [*Suhayda*, 1972, 1974; *Huntley*, 1976] the beach profiles were modeled as one or two plane slopes so the (implicit) smoothing scale is large, except at the slope break. The question of appropriate smoothing scales only explicitly arises when numerical solutions are attempted on topographies with relatively closely spaced survey points and a beach slope which varies rapidly near the origin. *Homan and Bowen* [1979] found better agreement between numerical solutions and the data of *Huntley* [1976] when the actual slope of a steep shoreface berm was reduced almost to that occurring further offshore. As they suggest, they may be due to cobbles on the foreshore but it may also indicate the necessity of smoothing the beach slope variations.

Mei and Le Mehaute [1966, equation 13] suggest that rapidly varying beach slopes are incompatible with the derivation of (1). It is clear that if u_x is discontinuous, as occurs at slope discontinuities, then neglected nonlinear terms such as uu_x are locally large, as are neglected linear terms which involve high order cross-shore derivatives. We have been unable to theoretially justify the present (or any other) smoothing scheme. Although of little importance to the present work, the choice

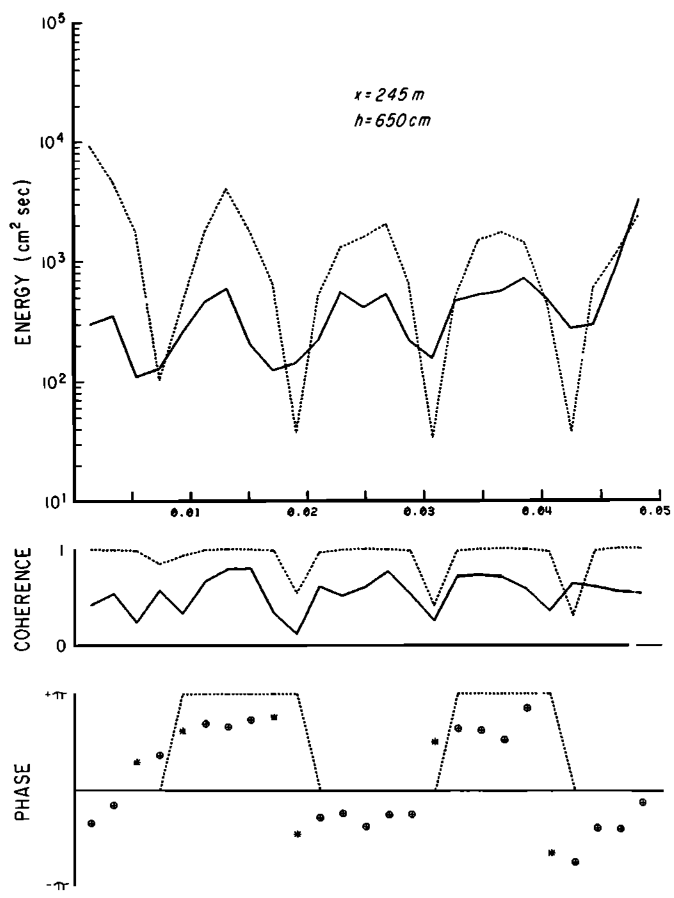

Fig. 5. Predicted (dashed line) and observed (solid line) energy spectra, coherence, and phase at the offshore (depth = 650 cm, $x = 245$ m) pressure sensor; February 11, 1981, Marine Street, $\Delta x = 40$ m, d.f. = 16. Coherence and phase are with the run-up sensor.

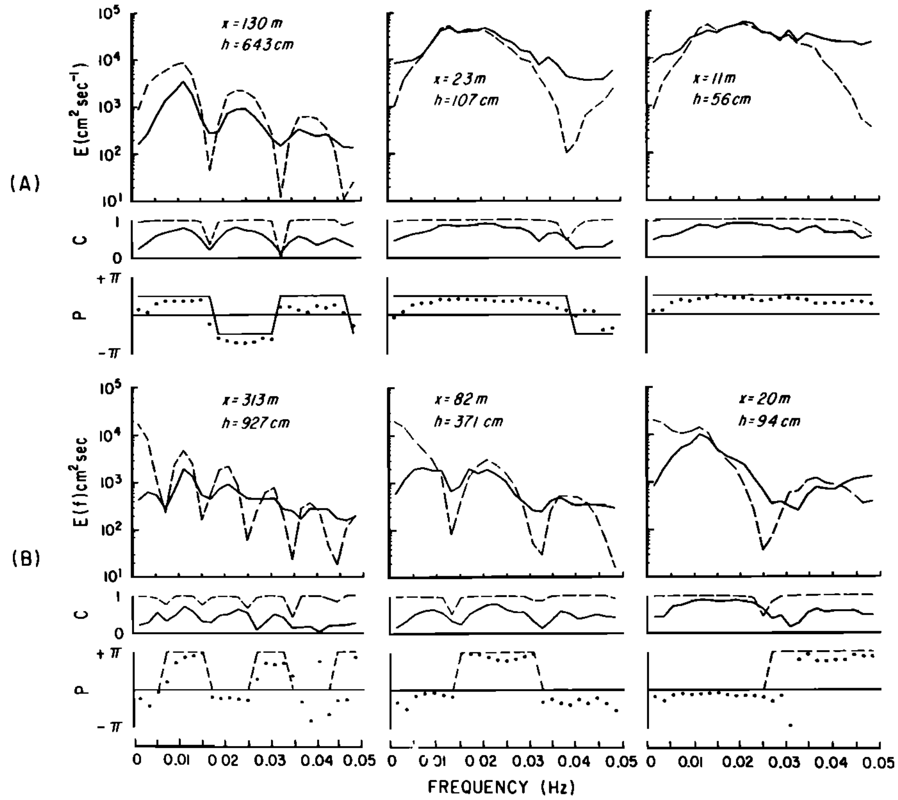

Fig. 6. Predicted (dashed line) and observed (solid line) cross-shore current (*a*) and elevation (*b*) spectra, coherence and phase at various depths (*h*) and average offshore distances (*x*); February 4, Santa Barbara, $\Delta x = 40$ m, d.f. = 60. Coherence and phase are with the run-up sensor.

of smoothing scales could be critical in some applications (i.e., the effect of changing beach face morphology on surf beat).

Observations

The run-up meter was used to obtain the Fourier coefficients of vertical run-up. This information, coupled with the numerical integrations of (1) yields predictions of the surf beat velocity and elevation fields at offshore locations. In order to allow for the motion of the mean shoreline location with tide, long data records of run-up were broken up into 17.1 min segments. Each segment was detrended and tapered in the time domain with a Kaiser-Bessel window [*Harris*, 1969] and then Fourier transformed. Because successive 17.1 min segments had different mean shoreline locations, the distance from the origin to a given sensor also varied, and was accounted for in the model. An integration was run for each 17.1 min segment, using the mean shoreline locations and observed run-up for the segment. Finally, the predicted cross-spectra from successive 17.1 min segments were averaged together, yielding predictions of coherence, phase and spectra for a given sensor at all frequencies (Figures 5–7), or at varying location for fixed frequency (Figures 8 and 9). Coherences and phases shown are between the run-up and offshore sensors. The different mean shoreline locations used in each 17.1 min piece result in slightly different predicted offshore locations of nodes and antinodes. The averaging of 17.1 min pieces results in nonzero spectral values, and low coherences, around nodal frequencies (Figures 5–9).

Model-data comparisons were done for each of the 27 data runs when the run-up meter was working (Table 1). Detailed results from each beach during runs with similar incident wave heights (80–90 cm) are presented here. Figure 4 shows that the run-up spectra from the different beaches have similar shapes. The apparent insensitivity of surf beat run-up spectral levels to substantial variations in the topography (Figure 1) is surprising. As in Figure 4, energetic peaks were not present in most of the surf beat run-up spectra, which suggests that the generation mechanism for surf beat does not have strong frequency selection on these unbarred beaches with no substantial nearby longshore barriers. Figure 5 shows the observed and predicted low frequency spectra at the only offshore sensor at Marine Street. Comparisons with a few of the many available sensors at the other sites are shown in Figures 6 and 7. The theoretical coherence between the run-up meter and an offshore sensor can be reduced near nodal frequencies of the offshore sensor (spectral valleys in Figures 5–7) if tidally induced changes in the mean shoreline location result in a predicted 180° phase shift (at fixed frequency and sensor) during a long data run. Since the data are analyzed in 17.1 min segments, the phase shift results in a decreased theoretical coherence. Note that the present frequency resolution is not adequate to fully describe the shape of the theoretical coherence valleys. Nevertheless, Figures 5–7 suggest that the tidally induced drift of node locations contributes to the sharp drops in observed coherence. However, coherence values at nodes would also be lowered (even in the absence of tides) by the presence of some progressive waves. Progressive waves would also contribute energy at standing wave nodes, and the observed power spectra are indeed smoother (i.e., less difference between peak and trough values) than predicted. Coefficients of reflection can be computed [*Suhayda*, 1972, 1974] but several arbitrary modeling assumptions are required. Similar cal-

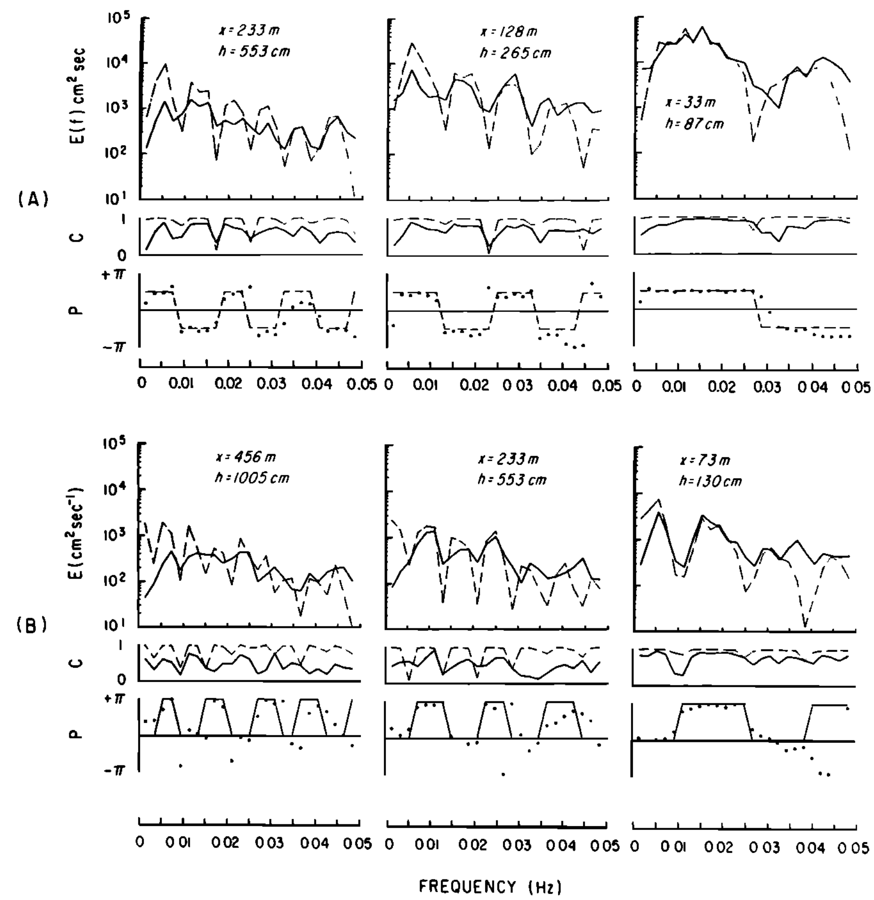

Fig. 7. Same as Figure 6 except November 21, Torrey Pines, d.f. = 16, Δx = 40 m.

culations suggest coefficients of reflection of very roughly 0.5 for the present data.

The agreement between predicted and observed phases and spectral hills and valleys is best in shallow water. At the deeper sensors (for example, Figure 7, h = 1005 cm) the frequency separation between predicted nodal frequencies is not much greater than the spectral resolution; as a result the spectral valleys are usually not well resolved. The number of phase jumps in Figures 5–7 provides information about the minimum edge wave mode number which would give results similar to the leaky wave solution used here. The lowest frequencies could have the lowest mode numbers. For example, at the h = 265 cm, x = 128 m velocity sensor at Torrey Pines (Figure 7, lower center panel), 0.02 Hz waves must be mode 1 or higher, while 0.04 Hz waves must be mode 3 or higher. Figures 8 and 9 show model-data (February 4 and November 21) comparisons for fixed frequencies (separated by 0.0039 Hz) with varying offshore distance. As in Figures 5–7, the model is based on the measured run-up coupled with the numerical solutions.

Observed and predicted band passed variances (frequency range 0.005 Hz $< f <$ 0.035 Hz) indicate a rather rapid decay of surf beat elevation and velocity energy with increasing offshore distance (Figure 10). The offshore decay in Figure 10 is smooth, compared to offshore dependence of the variance in the narrow frequency bands shown in Figures 8 and 9, because the band width 0.005 $< f <$ 0.035 Hz contains such a wide range of wavelengths that the nodes are not clustered at any particular location.

The amount of agreement between the standing wave model and observations illustrated in Figures 5–10 is typical of the present results. As in Figures 5–7, there were always phase jumps and coherence drops near the predicted nodal locations for frequencies less than 0.04 Hz. On a few days when long period swell was present, waves in the range 0.04 $< f <$ 0.05 Hz showed phase behavior that was obviously more consistent with progressive incoming waves. As in Figure 10 (lower right hand panel), the model always overpredicted (by about a factor of 2) the amount of surf beat elevation variance at offshore sensors at Santa Barbara. At Torrey Pines the cross-shore variation of elevation variance was usually better predicted (Figure 10, lower left hand panel) although underprediction by as much as a factor of 2 occurred on a few days. As in Figure 10 (upper panels), the predicted and observed velocity fields at both beaches usually showed good agreement near the shoreline (x < 100 m). The deeper velocity sensors always showed a marked overprediction of variance. Overprediction at offshore locations is consistent with the presence of some low mode edge wave energy. The day to day consistency of model-data comparisons at each beach are noteworthy. Although the surf beat energy levels varied greatly (Figure 2), the level of agreement between the data and the standing wave model did not. Figures 5–10 are typical of all data runs.

Although the agreement between the standing wave model and data is only qualitative (note the logarithmic scales on Figures 5–10), inferences can be made about generation mechanisms for surf beat. First, it is very unlikely that surf beat (as defined in this study) is simply a long wind wave generated by

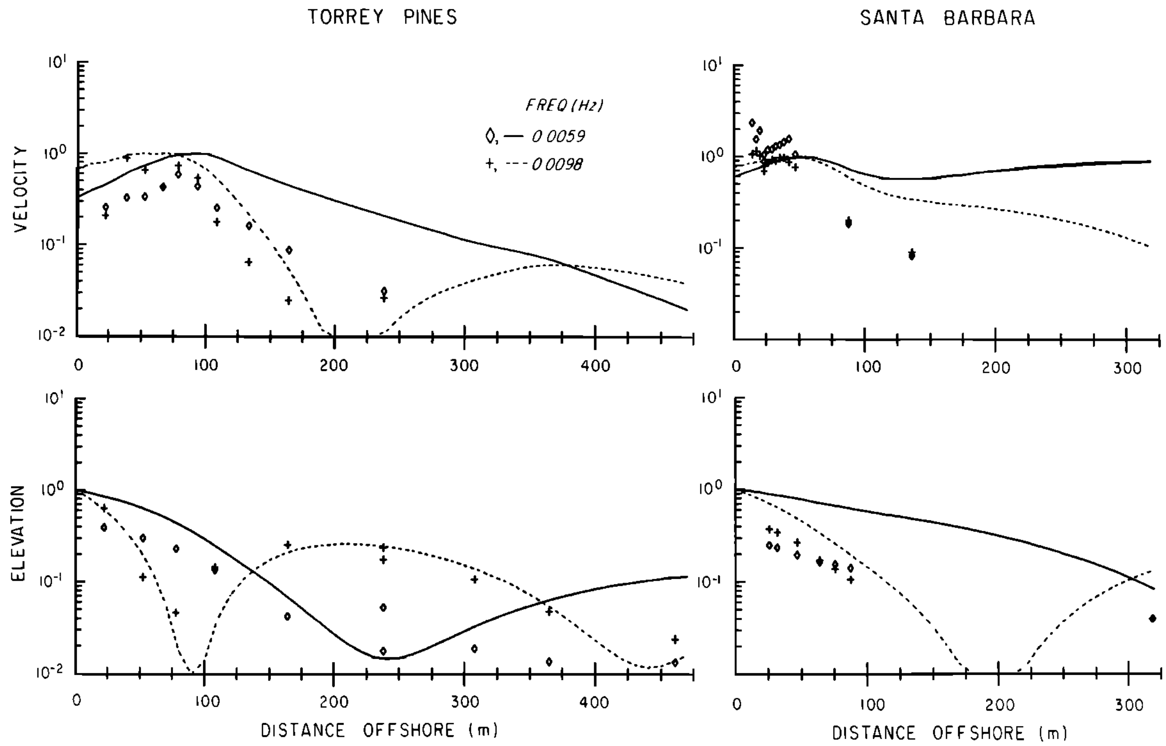

Fig. 8. Observed (triangles and crosses) and predicted (dashed and solid lines) normalized energy levels for two fixed frequencies (0.0059, 0.0098 Hz) as a function of offshore distance. Torrey Pines data (November 21) is shown in the left-hand panels, Santa Barbara (February 4) on the right, velocity in the upper panels, and elevation in the lower. All values are normalized by the maximum theoretical energy; $\Delta x = 40$ m.

and propagating away from storms, because surf beat energy levels are correlated with the variance at higher frequencies. If what we have identified as surf beat was a free wind wave, it would have appeared as a forerunner, a characteristic looked for and not found in this data set. The predominantly standing wave character of these observations is inconsistent with the hypothesis that surf beat is primarily generated by bore-bore capture within the surf zone (as hypothesized by *Bradshaw*

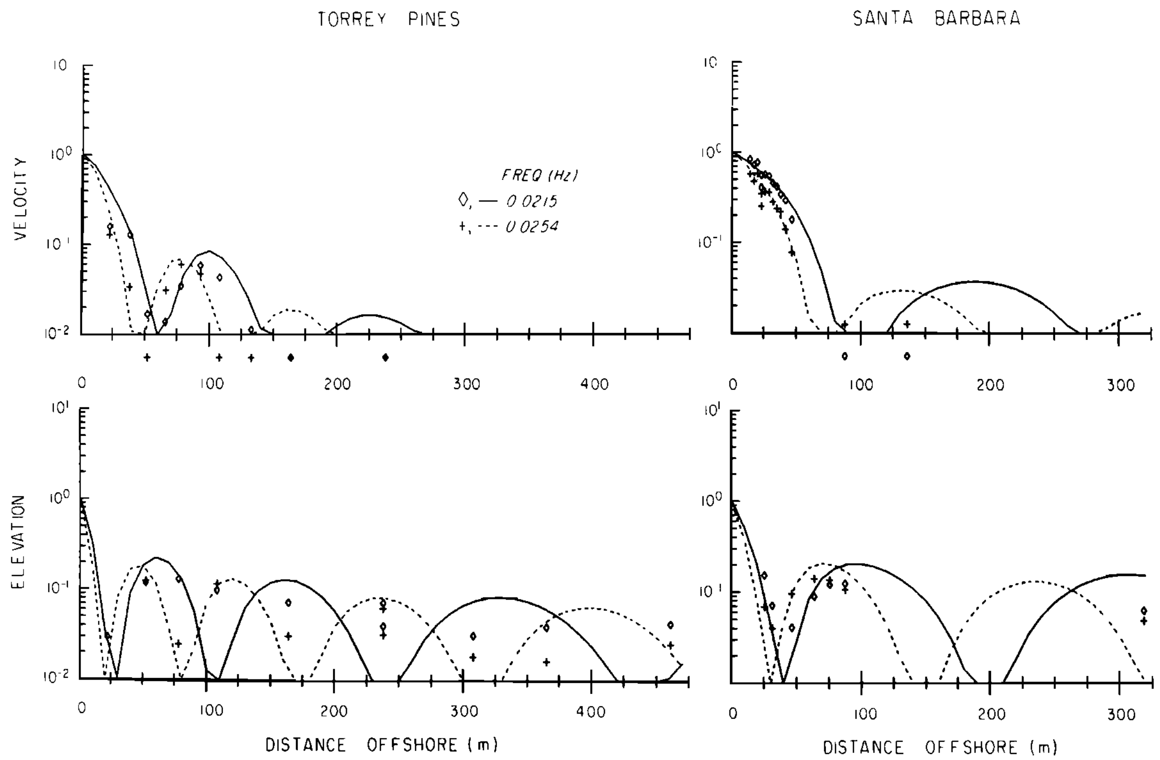

Fig. 9. Same as Figure 8 except frequencies are 0.021, 0.025 Hz. Points shown below the distance axis have values less than 10^{-2}.

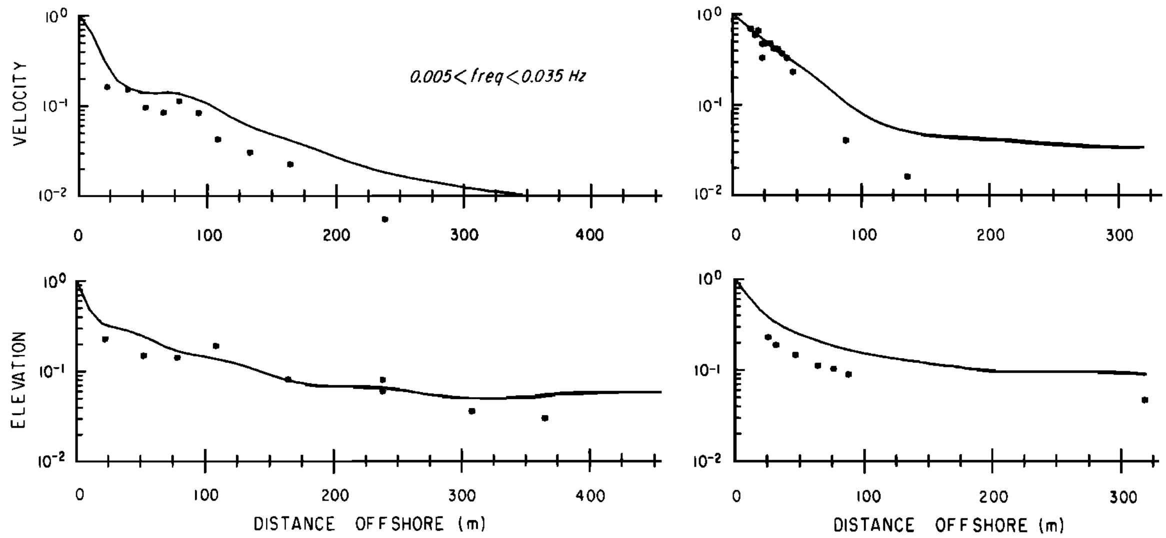

Fig. 10. Predicted (solid lines) and observed (asterisks) variance in the frequency range $0.005 < f < 0.035$ Hz; $\Delta x = 40$ m. Upper panels are velocity; lower panels are elevation.

[1980] and others) because bore-bore capture models predict no incoming surf beat energy outside the surf zone, and a gradual modification of the surf beat spectrum as more bores are captured. No such gradual spectral red shifting is observed. *Longuet-Higgins and Stewart* [1962] suggested theoretically that the shoreward propagating component of surf beat could be a locally forced response to incoming wave groups. For various reasons, one of which is that their model is only valid for small Ursell number, Longuet-Higgins and Stewart called their model "very crude." An alternative mechanism for generating incoming, leaky surf beat is resonant triad interactions between wind wave components of nearly equal frequency, a formalism valid for $O(1)$ Ursell numbers [*Freilich and Guza*, 1984]. Regardless of the details of the mechanism by which incoming wind wave modulations generate incoming surf beat, the reflection of this wave near the shoreline should produce something like a standing wave, consistent with the observations. The model of *Symonds et al.* [1982] hypothesizes that surf beat is the superposition of an incoming forced component [*Longuet-Higgins and Stewart*, 1962] and an outgoing wave generated by variations of surf zone width. The *Symonds et al.* [1982] prediction that the relative importance of these incoming and outgoing components will be a function of frequency and offshore distance seems inconsistent with the observation that the waves are primarily standing at all low frequencies and sensor positions. However, given the qualitative nature of the present discussion, no definitive statements can be made about the importance of fluctations in surf zone width to surf beat generation. *Gallagher* [1971] suggested that surf beat is composed of resonantly excited edge waves. The present cross-shore velocity and elevation data are consistent with the presence of high mode edge waves, as are the results from longshore arrays of current meters at Torrey Pines [*Huntley et al.*, 1981] and Santa Barbara (J. Oltman-Shay, personal communication, 1984). In principal, both longshore and cross-shore arrays and velocity components could be used to solve for the amplitudes of individual edge wave modes and for the relative amounts of incoming and outgoing resonantly and nonresonantly forced leaky waves. The analysis of all the available data on each day within the framework of a single model including all types of motion is clearly desirable. However, such a model does not presently exist, and it seems dauntingly difficult to construct. Notable theoretical problems are the inclusion of a realistic and stochastic incident wave field, the choice of topographic smoothing scales both in the cross-shore and longshore directions, the possibility that up

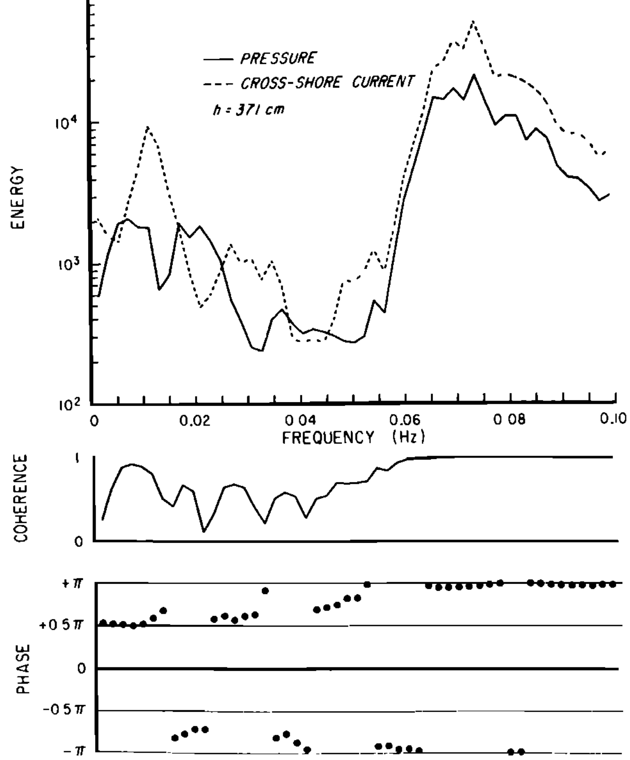

Fig. 11. Spectra, coherence, and phase for pressure and cross-shore current measured on February 4, 1980, at Santa Barbara; $x = 82$ m, $h = 371$ cm, d.f. = 60. Energy units are cm^2 s for pressure and $cm^2\ s^{-1}$ for current.

and down coast propagating edge waves do not have completely independent phases, the possibility of some forcing of surf beat both within and outside the surf zone, and the modeling of the spatial form of incompletely reflected waves.

The standing component of surf beat leads to peaks in the spectra at offshore locations (Figures 5–7). The peaks do not indicate any sort of preferential excitation of particular surf beat frequencies, as pointed out by *Holman* [1981] and others. This point is further illustrated by Figure 11, which shows the spectra and relative phase of co-located pressure and current fluctuations. For frequencies less than about 0.04 Hz, peaks in the pressure spectra correspond to valleys in the elevation spectra, and vice-versa. This is expected for standing waves, as are the phase jumps between approximately $\pm\pi/2$ which occur at nodal frequencies. For frequencies above about 0.03 Hz there are increasingly significant departures from a phase of $\pm\pi/2$, and above about 0.05 Hz the phase of $\pm\pi$ is indicative of shoreward propagating progressive waves. Several authors, most recently *Meadows et al.* [1982], have considered spectral peaks at surf beat frequencies, at a single sensor, to indicate that those frequencies are preferentially excited. Clearly this would be a wrong conclusion for the present data set.

Standing wave soltuions on a plane beach have properties roughly consistent with the observed ratios of surf beat velocity to elevation energy at various offshore depths. Away from the immediate vicinity of the shoreline ($X \gg 1$, where $X = (\sigma^2 x/g\beta)^{1/2}$) the spatial variation of the solutions is given by

$$\eta = a(\pi X)^{-1/2} \cos\left(2X - \frac{\pi}{4}\right) \tag{6a}$$

$$u = a\sigma(\beta X)^{-1}(\pi X)^{-1/2} \cos\left(2X - \frac{3\pi}{4}\right) \tag{6b}$$

Neglecting the nodal structure given by the cosine terms, as is appropriate when considering a relatively wide band width (Figure 10), yields

$$\frac{U_s(x)}{H_s(x)} = \left|\frac{\langle u^2(x)\rangle}{\langle \eta^2(x)\rangle}\right|^{1/2} = \left|\frac{g}{h}\right|^{1/2} \tag{7}$$

with angle brackets indicating the low passed variance. At the shoreline, $X = 0$, from (4).

$$\left|\frac{\langle u^2(0)\rangle}{\langle \eta^2(0)\rangle}\right|^{1/2} = \frac{\sigma}{\beta} \tag{8}$$

From Table 2 the observed ratios

$$\frac{U^{0,1}}{\eta^{0,1}} = 3.21 \qquad \frac{U^{1,2}}{\eta^{1,2}} = 2.7 \tag{9}$$

decrease with increasing depth, in agreement with (7). Equating the observed ratios (9) to $(g/\hat{h})^{1/2}$, as suggested by (7), yields

$$\hat{h}^{0,1} = 95 \text{ cm} \qquad \hat{h}^{1,2} = 134 \text{ cm} \tag{10}$$

The very simple (7) is seen to be qualitatively correct. Of course, more accurate theoretical results follow from the numerical solutions.

Integrating (8) over frequency, and assuming the spectrum is white over the frequency range 0–0.05 Hz, yields the ratio of shoreline values

$$\frac{\langle u^2(0)\rangle^{1/2}}{\langle \eta^2(0)\rangle^{1/2}} = 0.049\ \beta^{-1}\ \text{s}^{-1} \tag{11}$$

The β dependence in (11) may partially explain why $U^{0,1}$ is not well correlated with H_s^{inc}, compared with the correlation of R_s^v and H_s^{inc} (Table 2). If the shoreline elevation fluctuations (R_s^v) depend linearly on H_s^{inc} (independent of β), the velocity fluctuations at the shoreline should have a β dependence, thus reducing the correlation with H_s^{inc}. There may be some beach slope effect in the $U^{0,1}$ data set, particularly the points collected in the upper swash.

The more rapid seaward decay of the surf beat velocity field, compared with the elevation field (Figure 10), is consistent with (6), which predicts X^{-1} and X^{-3} decays for elevation and velocity energies. Note also that since $X^2 \sim x/\beta \sim h/\beta^2$ the attenuation at fixed depth or distance, compared to shoreline values, is relatively greater on a gentle beach than on a steep one. On a plane beach it would clearly be more sensible to use X values to characterize variances, rather than depths as is done here. However, on beaches which are not planar there is no simple variable corresponding to X.

Acknowledgments. The analysis was supported by the Office of Naval Research, Coastal Sciences Branch, under contracts N00014-75-C-0300 (R.T.G.) and NR 388-114 (E.B.T.). The data collection was supported by ONR and the Sea Grant Nearshore Sediment Transport Study (Project R/CA-N-40). R. J. Seymour obtained the bathymetric data at Torrey Pines and Santa Barbara. D. L. Inman provided the offshore survey at Marine Street. R. L. Lowe was the principal engineer, and many others contributed substantially, during the Santa Barbara and Torrey Pines experiments. Mike Clifton collected the Marine Street data. Valuable comments by reviewers are much appreciated.

REFERENCES

Bradshaw, M. P., Topographic control of run-up variability, *Proc. Coastal Eng. Conf., 17th*, 1091–1105, 1980.
Eckart, C., Surface waves on water of variable depth, *Wave Rep. 100*, 99 pp., Univ. of Calif., Scripps Inst. of Oceanogr., La Jolla, 1951.
Emery, K. O., and J. F. Gale, Swash and swash marks, *Eos Trans. AGU, 32*(1), 32–36, 1951.
Freilich, M. H., and R. T. Guza, Nonlinear effects on shoaling surface gravity waves, *Philos. Trans. R. Soc. London Ser. A, 311*, 1–41, 1984.
Gallagher, B., Generation of surf beat by non-linear wave interactions, *J. Fluid Mech., 49*, 1–20, 1971.
Goda, Y., Irregular wave deformation in the surf zone, *Coastal Eng. Jpn., 18*, 13–27, 1975.
Guza, R. T., Comment on 'Standing waves on beaches' by J. N. Suhayda, *J. Geophys. Res., 79*(36), 5671–5672, 1974.
Guza, R. T., and E. B. Thornton, Local and shoaled comparisons of sea surface elevations, pressures and velocities, *J. Geophys. Res., 85*(C3), 1524–1530, 1980.
Guza, R. T., and E. B. Thornton, Swash oscillations on a natural beach, *J. Geophys. Res., 87*(C1), 483–491, 1982.
Harris, F. J., Windows, harmonic analysis, and the discrete Fourier transform, *Rep. NUC TP532*, Nav. Undersea Center, San Diego, Calif., 1969.
Holman, R. A., Infragravity energy in the surf zone, *J. Geophys. Res., 86*(C7), 6442–6450, 1981.
Holman, R. A., and A. J. Bowen, Edge waves on complex beach profiles, *J. Geophys. Res., 84*(C10), 6339–6346, 1979.
Holman, R. A., and R. T. Guza, Measuring run-up on a natural beach, *Coastal Eng., 8*, 129–140, 1984.
Holman, R. A., and A. H. Sallenger, Jr., Set-up and swash on a natural beach, *J. Geophys. Res.*, in press, 1984.
Huntley, D. A., Long period waves on a natural beach, *J. Geophys. Res., 81*(36), 6441–6449, 1976.
Huntley, D. A., and A. J. Bowen, Comparison of the hydrodynamics of steep and shallow beaches, in *Nearshore Sediment Dynamics and Sedimentation*, edited by J. Hails and A. Carr, pp. 69–109, John Wiley, New York, 1975.
Huntley, D. A., R. T. Guza, and E. B. Thornton, Field observations of surf beat, 1, Progressive edge waves, *J. Geophys. Res., 86*, 6451–6466, 1981.
Inman, D. L., Mechanics of sediment transport by waves and currents, *SIO Ref. Ser. 68-10*, 6 pp., Scripps Inst. of Oceanogr., La Jolla, Calif., 1968*a*.

Inman, D. L., Mechanics of sediment transport by waves and currents, *SIO Ref. Ser. 68-26*, 9 pp., Scripps Inst. of Oceanogr., La Jolla Calif., 1968*b*.

Lamb, H., *Hydrodynamics*, 6th ed., 738 pp., Dover, New York, 1932.

Longuet-Higgins, M. S., and R. W. Stewart, Radiation stress and mass transport in gravity waves, with application to surf-beats, *J. Fluid Mech., 13*, 481–504, 1962.

Meadows, G. A., R. A. Shuchman, and J. D. Lyden, Analysis of remotely sensed long-period wave motions, *J. Geophys. Res., 87*(C8), 5731–5740, 1982.

Mei, C. C., and B. Le Mehaute, Note on the equations of long waves over an uneven bottom, *J. Geophys. Res., 71*, 393–400, 1966.

Munk, W. H., Surf beats, *Eos Trans. AGU, 30*, 849–854, 1949.

Sasaki, T., and K. Horikawa, Nearshore current system on gently sloping bottom, *Coastal Eng. Jpn., 18*, 123–142, 1975.

Sasaki, T., and K. Horikawa, Observation of nearshore current and edge waves, *Proc. Coastal Eng. Conf., 16th*, 791–809, 1978.

Sasaki, T., K. Horikawa, and S. Hotta, Nearshore current on a gently sloping beach, *Proc. Coastal Eng. Conf., 15th*, 626–644, 1976.

Sonu, C. J., N. Pettigrew, and R. G. Fredericks, Measurement of swash profile and orbital motion on the beach, in *Ocean Wave Measurement and Analysis*, vol. 1, pp. 621–638, American Society of Civil Engineers.

Stoer, J., Extrapolation methods for the solution of initial value problems and their practical realization, *Lecture Notes Math., 362*, 1972.

Suhayda, J. N., Experimental study of the shoaling transformation of waves on a sloping bottom, Ph.D. dissertation, Scripps Inst. of Oceanogr., La Jolla, Calif., 1972.

Suhayda, J. N., Standing waves on beaches, *J. Geophys. Res., 72*(21), 3065–3071, 1974.

Symonds, G., D. A. Huntley, and A. J. Bowen, Two-dimensional surf beat: Long wave generation by a time-varying breakpoint, *J. Geophys. Res., 87*(C1), 492–498, 1982.

Thornton, E. B., and R. T. Guza, Energy saturation and phase speeds measured on a natural beach, *J. Geophys. Res., 87*(C12), 9499–9508, 1982.

Thornton, E. B., and R. T. Guza, Transformation of wave height distribution, *J. Geophys. Res., 88*(C10), 5925–5938, 1983.

Tucker, M. J., Surf beats: Sea waves of 1 to 5 minute period, *Proc. R. Soc. London Ser. A, 202*, 565–573, 1950.

Wright, L. D., B. G. Thom, and J. Chappell, Morphological variability of high energy beaches, *Proc. Coastal Eng. Conf., 16th*, 1180–1194, 1978.

Wright, L. D., J. Chappel, B. G. Thom, M. P. Bradshaw, and P. J. Cowell, Morphodynamics of reflective and dissipative beach and inshore systems: Southeastern Australia, *Mar. Geol., 32*, 105–140, 1979.

Wright, L. D., R. T. Guza, and A. D. Short, Surf zone dynamics on a high energy dissipative beach, *Mar. Geol., 45*, 41–62, 1982.

R. T. Guza, Shore Processes Laboratory, A-009, Scripps Institution of Oceanography, University of California at San Diego, La Jolla, CA 92093.

E. B Thornton, Naval Postgraduate School, Monterey, CA 93940.

(Received June 4, 1984;
accepted July 25, 1984.)